Programmable transdermal drug delivery of nicotine using carbon nanotube membranes

Ji Wu[a], Kalpana S. Paudel[b], Caroline Strasinger[b], Dana Hammell[b], Audra L. Stinchcomb[b,1], and Bruce J. Hinds[a,1]

[a]Chemical and Materials Engineering Department, University of Kentucky, Lexington, KY 40506; and [b]College of Pharmacy, University of Kentucky, Lexington, KY 40536

Edited by Mildred Dresselhaus, Massachusetts Institute of Technology, Cambridge, MA, and approved May 13, 2010 (received for review April 8, 2010)

Carbon nanotube (CNT) membranes were employed as the active element of a switchable transdermal drug delivery device that can facilitate more effective treatments of drug abuse and addiction. Due to the dramatically fast flow through CNT cores, high charge density, and small pore dimensions, highly efficient electrophoretic pumping through functionalized CNT membrane was achieved. These membranes were integrated with a nicotine formulation to obtain switchable transdermal nicotine delivery rates on human skin (in vitro) and are consistent with a Fickian diffusion in series model. The transdermal nicotine delivery device was able to successfully switch between high (1.3 ± 0.65 μmol/hr-cm^2) and low (0.33 ± 0.22 μmol/hr-cm^2) fluxes that coincide with therapeutic demand levels for nicotine cessation treatment. These highly energy efficient programmable devices with minimal skin irritation and no skin barrier disruption would open an avenue for single application long-wear patches for therapies that require variable or programmable delivery rates.

electroosmosis | electrophoresis | smoking cessation | medical device

Presently there are 19 drugs and drug combinations that have been approved by the Food and Drug Administration for transdermal drug delivery (TDD) (1). Compared to traditional oral and injectable drug delivery routes, TDD systems have many advantages including painless application, self-administration, controlled release delivery, and avoidance of degradation in the gastrointestinal tract and the first-pass effect of the liver (2). One of the most important areas of TDD application is in addiction treatment, because the overall costs of drug abuse in the United States exceed half a trillion dollars annually as reported by the National Institute on Drug Abuse (NIDA) (3). Nicotine TDD has been widely used for smoking cessation programs. However, these traditional transdermal patches cannot provide variable drug delivery rates, resulting in less successful drug withdrawal treatment (4–6). Variable rate delivery is also required in pain treatment, where patient controlled on-demand delivery is required as well as limits imposed by physicians to prevent inadvertent overdose. Although iontophoresis TDD has the capability to provide variable and programmable delivery rates, it requires a strong electric current across human skin, which can cause serious skin irritation (7) and has high power requirements. High power requirements make miniaturization difficult and require frequent battery changes. A new programmable TDD technology is required that can adjust dosing as prescribed by a physician and as patient need changes, and have small power requirements for compact device design. Recently carbon nanotube (CNT) membranes have been a subject of considerable research activity (8–12). In general, there are three key attributes unique to CNT membranes. First, CNTs have atomically smooth graphitic cores that allow 10,000× faster fluid flow as compared to classical materials (9). Second, functional chemistry introduced during the CNT tip opening process (H_2O plasma oxidation) provides gate-keeping molecules (9, 11). Last, carbon nanotubes are conductive allowing for efficient electrochemical functionalization and electroosmosis pumping (8, 13). In conventional membrane materials, elecotroosmosis is an inherently inefficient process with high power requirements to achieve usable fluxes. However, the nearly perfect slip boundary layer, as indicated by a 10,000-fold increase in fluid flow, and small diameters of CNTs, within the electrochemical Debye screening length, can allow for highly efficient electrophoretic pumping at rates that can be applied to programmable TDD. Herein, we show the incorporation of switchable carbon nanotube membranes into a transdermal nicotine system on human skin in vitro. Nicotine is electrophoretically pumped at low power (12 d battery life) across the CNT membrane at rates necessary for nicotine replacement therapy.

Results and Discussion

Carbon nanotube membranes were fabricated using a microtome-cutting method similar to the one reported by Crooks and coworkers (14). Our variation from this precedent was to use high CNT loadings (5–10%) of either multiwalled (MWCNT) or double-walled (DWCNT) CNTs for increased pore area. To obtain efficient electroosmosis pumping, MWCNT membranes were further functionalized with negatively charged dye molecules that have four sulphonate ($-SO_3^-$) groups using a two-step process (Fig. 1*C*). The first step involves electrochemical diazonium grafting that generates a uniform monolayer of polybenzoic acid (8, 15), which was further coupled to Direct Blue 71 dye via a carbodiimide coupling reaction resulting in a quadrupled charge density. It should be pointed out that a high charge density on the surface of CNTs is necessary to get efficient electroosmosis pumping because it will determine how many counter ions could be adsorbed to pump neutral molecules (16, 17). The functionalized CNT membranes were characterized using electrochemical impedance spectroscopy (EIS). It was found that charge transfer resistance (R_{et}) increased dramatically from 200 to approximately 300 ohms after diazonium grafting and dye coupling reaction, which is consistent with an increased negative surface charge density (18, 19) repelling anionic iron hexacyanide. The observed electroosmosis velocity of functionalized CNT membrane is as high as 0.05 cm/s applying a −300 mV bias. In terms of pumping the same amount of neutral molecules, the energy consumption of our CNT membranes are nearly 50× less than for electroosmosis through nanocarbon membranes reported earlier by Martin and coworkers (13). This apparent difference in efficiency is attributed to the composition and size of membrane materials. The prior membranes were made of noncrystalline CNTs with a 120 nm inner diameter, whereas the present membranes are fabricated using crystalline CNTs with a 7 nm core diameter. Smaller inner diameter (higher ratio of surface area to mass) and an atomically smooth core are beneficial to an enhanced

Author contributions: A.L.S. and B.J.H. designed research; J.W., K.S.P., C.S., and D.H. performed research; J.W., K.S.P., D.H., A.L.S., and B.J.H. analyzed data; and J.W., C.S., and B.J.H. wrote the paper.

Conflict of interest statement: US Patent 7,229,556 (2007) issued to the University of Kentucky.

This article is a PNAS Direct Submission.

[1]To whom correspondence may be addressed. E-mail: bjhinds@engr.uky.edu or audra.stinchcomb@uky.edu.

www.pnas.org/cgi/doi/10.1073/pnas.1004714107

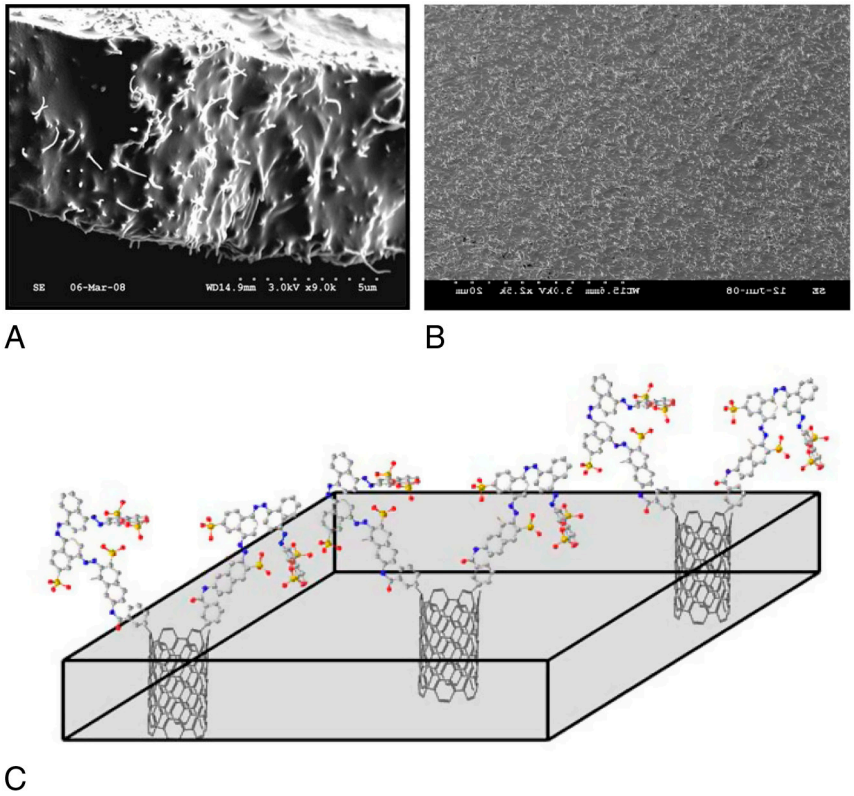

Fig. 1. SEM images of microtome-cut CNT membrane (*A*) cross-sectional view and (*B*) top view; (*C*) schematic shows the molecular structure of the anionic dye covalently functionalized on the surface of CNTs (gray: C; red: O; blue: N; yellow: S).

electroosmosis velocity and electrophoretic efficiency. To further optimize the pumping efficiency, smaller DWCNTs were used with an inner diameter of <2 nm and functionalized with the charged dye molecule. As shown in Fig. 2*A* nicotine high and low flux-values through CNT membrane alone are 1.1 and 0.19 μmoles/hr.cm^2, respectively, using a pH 8 220 mM (35 mg/mL) nicotine donor solution. Usually electrophoretic flow is much faster than electroosmotic flow under electric field in the case of macroscopic channels. In nanoporous channels, however, electroosmotic flow is not negligible and could account for approximately 30% of total flow according to theoretical simulations (20). Nicotine is 50% cationic at pH8 and so electrophoresis would still be the dominate transport mechanism, whereas the contribution from electroosmosis is also significant and increases the power efficiency. With applied bias as small as −300 mV, the high/low nicotine flux ratio (5.5) exceeds the demand for nicotine cessation treatments (3.6) (21). Using typical pumping voltages of −0.6 V and 57 μA/cm^2, the power consumption of the CNT membrane is also highly favorable for compact devices. For a 25.8 cm^2 (commercially available size) nicotine transdermal patch made of a CNT membrane, a button cell battery with a capacity of 247 mWh can be pumping continuously for 12 d. Several patch products on the market are designed to wear 7 d at a time with acceptable levels of irritation (22).

A diffusion in series model was created to simulate switchable transdermal nicotine delivery using CNT membrane as the rate-limiting component. In this model, nicotine has to pass three layers of diffusion barrier before entering the saline receiver compartment (Fig. 2*B*). These three layers consist of 5 μm thick CNT membrane, 140 μm thick 2% hydroxyethylcellulose (HEC) gel and 200 μm thick human skin. Because the gel is mainly composed of water (98%) the diffusion coefficient is near bulk water, thus there is a minimal concentration gradient of nicotine within the gel. As reported by literature, there are only 3.3 water molecules bound to one HEC polymer repeating unit on average (23). In other words, there are >96% free water molecules in the case of 2% (wt/wt) HEC gel (molecular weight of HEC polymer repeating unit is 272).

The flux of nicotine in and out of the gel can be calculated using Fick's first law as shown in Eqs. **1** and **2**

$$J_{\text{in}} = D_{\text{CNTs}}(C_{\text{donor}}\text{-}C_{\text{gel}})/l_{\text{cnt}} \quad [1]$$

$$J_{\text{out}} = D_{\text{skin}}(C_{\text{gel}}\text{-}0)/l_{\text{skin}} \quad [2]$$

where J is flux, D_{CNTs} is diffusion coefficient for entire membrane area, D_{skin} is the effective diffusion coefficient for entire skin area and thickness, C_{donor} is donor concentration, C_{gel} is concentration of drug in the gel intermediate layer, l_{cnt} is thickness of CNT membrane, and l_{skin} is the thickness of skin sample. When pumping bias is applied to the CNT membrane, D_{CNTs} increases proportionately by the flux ratio. The nicotine concentration in receiver is negligible compared to the donor concentration, therefore creating sink conditions. Based on the Fick's law assumption that the average nicotine concentration in human skin is half of that in gel, the concentration change in the gel can be obtained from Eq. **3**

$$\Delta C_{\text{gel}} = (J_{\text{in}}\text{-}J_{\text{out}}) \times \Delta t/(l_{\text{gel}} + l_{\text{skin}}/2) \quad [3]$$

where ΔC_{gel} and Δt are the concentration change of nicotine in gel and the change in time, respectively. When the nicotine flux into and out of the gel is equal ($J_{\text{in}} = J_{\text{out}}$), a steady-state nicotine concentration (C_{ss}) in the gel is reached and can be calculated from Eq. **4**:

$$C_{\text{ss}} = C_{\text{donor}}/(1 + (l_{\text{cnt}}D_{\text{skin}}/D_{\text{cnt}}l_{\text{skin}})). \quad [4]$$

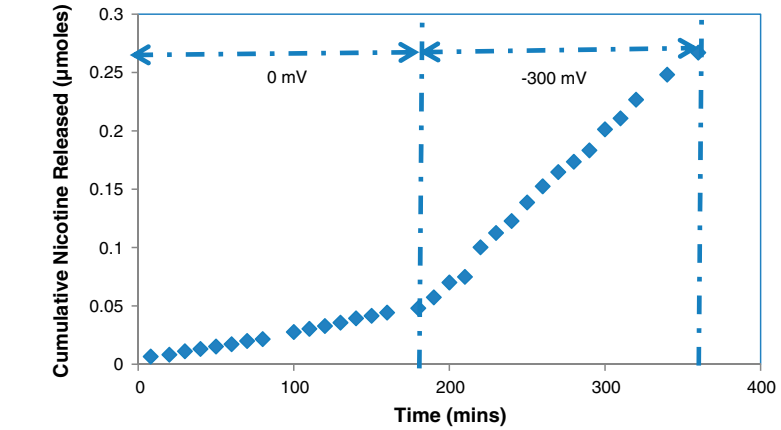

a)

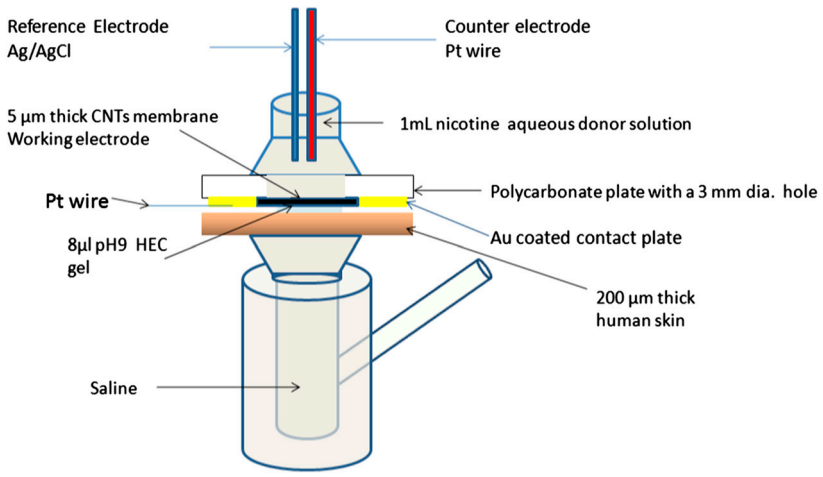

b)

Fig. 2. (*A*) Flux of nicotine through CNT membrane with/without applying a −300 mV bias. The ratio of −300 mV to 0 mV nicotine flux is 5.5. Donor solution is a pH8 220 mM (35 mg/mL) nicotine aqueous solution; (*B*) schematic for switchable transdermal drug delivery (skin/gel/CNT membrane). Active area of CNT membrane is 0.07 cm^2.

Once C_{ss} in the gel is obtained, steady-state nicotine flux can be calculated using either Eq. **1** or Eq. **2**. For an approximation, we can assume that steady-state rates will not be achieved until the nicotine concentration in skin reaches half of the steady-state concentration in gel, thus giving an estimation of lag time Eq. **4**:

$$\text{Lagtime}_{1/2} = (C_{ss}/2) \times (l_{gel} + l_{skin}/2)/((D_{CNTs}(C_{donor}\text{-}C_{ss}/2)/l_{cnt}). \quad \textbf{[5]}$$

Using the above model, it was found that switchable nicotine transdermal delivery cannot be realized if the permeability of human skin is higher than that of CNT membrane; otherwise human skin would become the rate-limiting component, and the permeability change of CNT membrane made via applying bias would have a minor impact on the final nicotine flux through human skin. Low skin diffusion coefficients also cause long lag times due to a higher nicotine equilibrium concentration in the gel, which is detrimental from a practical point of view (6, 24). The implication of this model is that drugs with high permeation rates, such as nicotine, or TDD enhancers such as microneedles (25) and prodrugs (26, 27) must be used. Nicotine can permeate through human skin quickly with a very small lag time due to its low molecular weight and other optimal physicochemical properties (28). Permeability of nicotine through human skin can be affected by many factors, such as age, location, hydration, and pH values as well (5). In general, higher pH values above the pKa can lead to higher nicotine permeability. Another important practical point of the above model is that overall dosing is limited by the CNT membrane, hence variation between CNT samples would dominate the variation between different patches. For our current laboratory-based process of CNT membrane fabrication ($n = 16$), the diffusion flux (feed of 5 mmol caffeine) was 4.9± 2.0 nmol/cm^2-hr. It is important to note that the CNT membranes fluxes are quickly screened by measuring ionic current across CNT membranes and can be performed in an automated sorting system prior to patch assembly. Also, the "on" flux is dictated by EO current that can be controlled by a constant current circuit, thus not rely on initial CNT permeability.

The required on and off flux values for nicotine cessation treatment can be calculated using Eq. **6** (21, 29)

$$J = C_{ss} \times CL/A \quad \textbf{[6]}$$

where J is the required therapeutic flux; C_{ss} is the steady-state nicotine concentration in plasma; CL is total body clearance (mL/ min); and A is membrane area. Using an approximately 14 cm^2 nicotine patch of commercially available size, the required high and low flux values should be 1.1 and 0.30 μmoles/ hr.cm^2, respectively for nicotine cessation treatment (21, 29). The peak and trough nicotine plasma concentrations and clearance value used for the flux calculation were 54 ng/mL, 15 ng/mL,

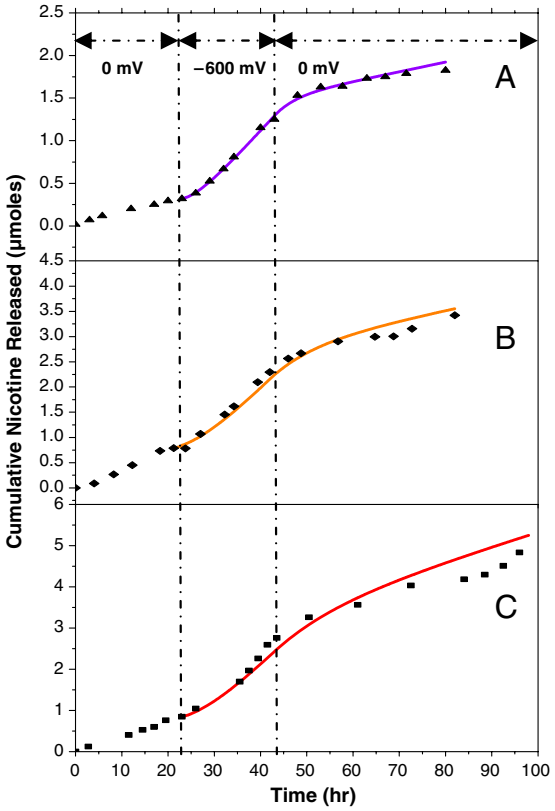

Fig. 3. Cumulative nicotine drug release from three CNTs/gel/human skin design using 0 and −600 mV biases. Different CNT membranes and skin samples were used for each experiment (*A*–*C*) with solid curves as simulated data and solid points as experimental data.

and 1200 mL/ min, respectively. The average smoker has a steady-state nicotine plasma concentration of about 10–20 ng/mL with peak levels reaching approximately 54 ng/mL throughout the day with each cigarette (21).

Switchable transdermal nicotine delivery was carried out using a modified Franz cell installed with 3 electrodes for applying bias (as shown in Fig. 2*B*). As shown with three different skin samples in Fig. 3, steady-state nicotine on-flux values can be reached in <6 h after applying a −600 mV bias, which can be turned off again approximately 10 h after switching to zero bias. The experimental data are very consistent with the simulated values (solid lines) derived from the diffusion in series model by numerically calculating Eq. **3** stepwise in time (1 min. steps). The diffusion coefficients for skin and CNT membrane are 2.68×10^{-8} cm^2/s and 1.07×10^{-10} cm^2/s, respectively. Table 1 shows the comparison of experimental, simulated, and required on/off nicotine flux and their ratios. The experimental ($n = 3$) high and low flux values are 1.3 ± 0.65 μmol/hr-cm^2 and 0.33 ± 0.22 μmol/hr-cm^2, respectively, and meet the demand for nicotine cessation treatments (1.1 and 0.30 μmoles/hr.cm^2). In general, a short lag time and predictable nicotine release at a therapeutically useful flux makes this device a desirable candidate for programmable nicotine cessation treatment. (21, 24).

In conclusion, the unique physical properties of CNT membranes allow highly efficient electrophoretic pumping and were utilized to control the delivery rates of an addictive drug for a programmable treatment device. The CNT membrane acted as the rate-limiting component and observed flux values are consistent with a simple diffusion in series model that is based on Fick's law. Power usage in the CNT membranes was reduced 50-fold allowing a common watch battery to operate for 12 d. The steady-state flux of nicotine met the demands for therapeutic smoking cessation treatment. This developed method is universal and can be applied to the delivery of other drugs used for substance abuse treatment, such as clonidine regimens used in opioid withdrawal. Programmable TDD devices can have significant impact in addiction treatment where variable dosing regimens are required.

Methods

Fabrication and Functionalization of CNT Membranes. MWCNTs with an average core diameter of approximately 7 nm were fabricated on quartz substrate via a chemical vapor deposition approach using ferrocene/xylene as the feeding gas (3). The length of MWCNTs ranges from 100–150 μm as measured by DekTak Profilometer. In the next step, MWCNTs were mixed thoroughly with Epon 862 epoxy resin (Miller Stephenson Chem. Co.), surfactant Triton-X 100 (Sigma Aldrich), and hardener methylhexahydrophthalic anhydride (MHHPA, Broadview Tech. Inc.) using a Thinky™ Mixer. The appropriately-cured CNTs-Epoxy composite was cut into approximately 5 μm thick membranes using a microtome equipped with a glass knife. The residual epoxy on the tips of CNTs was removed via H_2O plasma oxidation. DWCNTs (approximately 2 nm, Cheaptubes, Inc) membranes were prepared using a similar method as described above. The as-cut CNTs membranes were functionalized using a two-step process. In the first step, CNTs were grafted with benzoic acid through electrochemically reducing 5 mM 4-carboxy phenyl diazonium tetrafluoroborate in 0.1 M HCl and 0.1 M KCl electrolyte at −0.6 V for 4 min (8). The diazonium compound was synthesized following a method reported by Belanger and coworkers (30). Next, benzoic acid was coupled to Direct Blue 71 dye via a carbodiimide coupling reaction. Specifically, 10 mg 1-[3-(dimethylamino) propyl]-3-ethylcarbodiimide hydrochloride (EDC, 98%, Aldrich) was added to 4 mL of 50 mM Direct Blue 71 dye in 0.1 M 2-N-morphilino ethanesulfonic acid (MES, 99%, Sigma) buffer, and the reaction lasted for 12 h at ambient temperature, after which the membrane was rinsed thoroughly using 0.1 M MES buffer, 0.1 M KCl solution and deionized water to remove unreacted chemicals.

Characterization of CNTs Membrane. EIS measurements were employed to characterize the surface chemistry of CNTs membranes. Measurements were performed in the frequency range of 100 kHz – 0.2 Hz with a sinusoidal amplitude modulation of 10 mV using a Model 263A Potentiostat and FRD 100 Frequency Response Analyzer from Princeton Applied Research. Faradaic EIS

Table 1. Comparison of experimental and simulated on/off (−600 mV vs. 0 mV) nicotine fluxes and their ratios

Study	Nicotine flux (μmoles/hr.cm^2)	On (−600 mV)	Off (0 mV)	On/off ratio
Experiment 1	Observed	2.0	0.56	3.5
Experiment 2	Observed	1.2	0.29	4.3
Experiment 3	Observed	0.71	0.13	5.5
Average	Observed	1.3 ± 0.65	0.33 ± 0.22	4.4 ± 1.0
Experiment 1	Simulated	1.6	0.48	3.4
Experiment 2	Simulated	1.3	0.28	4.6
Experiment 3	Simulated	0.72	0.16	4.5
Average	Simulated	1.2 ± 0.49	0.31 ± 0.16	4.2 ± 0.67
Required flux	Calculated (see text)	1.1	0.30	3.6

The donor concentration used is 713 mM (116 mg/mL) pH8 nicotine aqueous solution, and the ionic strength is 0.35 M. Values reflect steady-state fluxes.

measurements were carried out at 230 mV using an electrolyte consisting of 5 mM $K_3Fe(CN)_6$ and $K_4Fe(CN)_6$, 0.1 M KCl, and 10 mM K_2CO_3 (pH10.8). S-4300 HITACHI Scanning Electron Microscope and JEOL 2010F Transmission Electron Microscope were used to examine the microstructure of as-cut CNTs membranes.

Preparation of Human Skin for Transdermal Nicotine Delivery Studies. Human skin harvested during abdominoplasty was used for the transdermal nicotine delivery studies and obtained from the Cooperative Human Tissue Network. Human tissue use was approved by the University of Kentucky Institutional Review Board. Human skin sections were prepared using a Padgett dermatome set to 200 μm and the human skin samples were stored at −20 °C before they were thawed to room temperature at the time of the experiment.

Switchable Transdermal Nicotine Delivery Studies. All transdermal nicotine delivery studies were carried out using a modified Franz cell that was equipped with three electrodes to apply bias on CNT membrane (Fig. 2*B*). CNT membrane, Ag/AgCl in saturated KCl solution and platinum wire were used as working, reference and counter electrodes, respectively. The CNT membrane is conductive with a resistivity of approximately 100 ohm-cm. Two percent HEC in pH 9 50 mM ammonium bicarbonate and ammonium hydroxide buffer solution was utilized between human skin and CNT membrane to provide good contact. The donor solution was pH 8, 0.7 M nicotine in deionized water, and the receiver was 0.9% saline. The transdermal nicotine delivery studies were carried out using a water bath of 37 °C, which gives a skin surface temperature of 33 °C. The area of CNT membrane was 0.07 cm^2, and the distance between working and counter electrodes was approximately 1 cm. The typical average transmembrane current was approximately 4×10^{-6} A while applying a −600 mV bias.

HPLC Analysis. All samples were analyzed by HPLC on a Waters 717plus autosampler, a 1525 Binary HPLC pump or a 600 pump and controller, a 2487 dual absorbance detector set at a wavelength of 259 nm utilizing Waters Breeze™ or Empower™ software. Additionally, a Brownlee (Perkin Elmer) C-18 reversed-phase Spheri-5 μm column (220 × 4.6 mm) with a NewGuard C-18 reversed-phase 7 μm guard column (15 × 3.2 mm) was used. The mobile phase consisted of 20 mM ammonium acetate (with 5% acetoniltrile): methanol (10:90) and flow rate of 1 mL/min. The injection volume was 20 μL, run time of 9–10 min, and the retention time of nicotine was 5.9–7.0 min. Diffusion samples were collected and prepared for analysis by mixing 1:1 diffusion sample:acetonitrile and placing the mixture in silanized HPLC vials.

ACKNOWLEDGMENTS. We thank Karen Gerstandt and Xin Su for helpful discussions. Rodney Andrews and Dalli Qian from the Center for Applied Energy, University of Kentucky supplied MWCNTs. Facility support was provided by the Center for Nanoscale Science and Engineering and Electron Microscopy Center at the University of Kentucky. Financial support from the National Institutes of Health (NIH) NIDA (R01DA018822) and National Science Foundation (0348544) is greatly appreciated by the authors. Human skin was obtained through the NIH-sponsored Cooperative Human Tissue Network.

1. Food and Drug Administration (2007) *Approved Drug Products with Therapeutic Equivalence Evaluations* (Department of Health and Human Services, Rockville, MD), 27th Ed.
2. Prausnitz MR, Langer R (2008) Transdermal drug delivery. *Nat Biotechnol* 26:1261–1268.
3. Manchikanti L (2007) National drug control policy and prescription drug abuse: Facts and fallacies. *Pain Physician* 10:399–424.
4. Wills S (2005) *Drugs of Abuse* (Pharmaceutical Press, London).
5. Prausnitz MR, Mitragotri S, Langer R (2004) Current status and future potential of transdermal drug delivery. *Nat Rev Drug Discov* 3:115–124.
6. Malin DH (2001) Nicotine dependence: Studies with a laboratory model. *Pharmacol Biochem Behav* 70:551–559.
7. Prausnitz MR (1996) The effects of electric current applied to skin: A review for transdermal drug delivery. *Adv Drug Deliver Rev* 18:395–425.
8. Majumder M, Zhan X, Andrews R, Hinds BJ (2007) Voltage gated carbon nanotube membranes. *Langmuir* 23:8624–8631.
9. Majumder M, Chopra N, Andrews R, Hinds BJ (2005) Nanoscale hydrodynamics: Enhanced flow in carbon nanotubes. *Nature* 438:44–44.
10. Kim S, Jinschek JR, Chen H, Sholl DS, Marand E (2007) Scalable fabrication of carbon nanotube/polymer nanocomposite membranes for high flux gas transport. *Nano Lett* 7:2806–2811.
11. Holt JK, et al. (2006) Fast mass transport through Sub-2-nanometer carbon nanotubes. *Science* 312:1034–1037.
12. Hinds BJ, et al. (2004) Aligned multiwalled carbon nanotube membranes. *Science* 303:62–65.
13. Miller SA, Young VY, Martin CR (2001) Electroosmotic flow in template-prepared carbon nanotube membranes. *J Am Chem Soc* 123:12335–12342.
14. Sun L, Crooks RM (2000) Single carbon nanotube membranes: A well-defined model for studying mass transport through nanoporous materials. *J Am Chem Soc* 122:12340–12345.
15. Bahr JL, et al. (2001) Functionalization of carbon nanotubes by electrochemical reduction of aryl diazonium salts: A bucky paper electrode. *J Am Chem Soc* 123:6536–6542.
16. Stone HA, Stroock AD, Ajdari A (2004) Engineering flows in small devices. *Annu Rev Fluid Mech* 36:381–411.
17. Chen Y, Ni Z, Wang G, Xu D, Li D (2008) Electroosmotic flow in nanotubes with high surface charge densities. *Nano Lett* 8:42–48.
18. Majumder M, et al. (2008) Enhanced electrostatic modulation of ionic diffusion through carbon nanotube membranes by diazonium grafting chemistry. *J Membr Sci* 316:89–96.
19. Katz E, Willner I (2003) Probing biomolecular interactions at conductive and semiconductive surfaces by impedance spectroscopy: Routes to impedimetric immunosensors, DNA-sensors, and enzyme biosensors. *Electroanal* 15:913–947.
20. Srinivasan V, Higuchi WI (1990) A model for iontophoresis incroporating the effect of convective solvent flow. *Int J Pharm* 60:133–138.
21. Feyerabend C, Ings RMJ, Russell MAH (1985) Nicotine pharmocokinetics and its application to intake from smoking. *Br J Clin Pharmac* 19:239–247.
22. Abrams LS, Skee DM, Natarajan J, Wong FA, Anderson GD (2002) Pharmacokinetics of a contraceptive patch (Evra (TM)/Ortho Evra (TM)) containing norelgestromin and ethinyloestradiol at four application sites. *Brit J Clin Pharmaco* 53:141–146.
23. Baumgartner S, Lahajnar G, Sepe A, Kristl J (2002) Investigation of the state and dynamics of water in hydrogels of cellulose ethers by 1 H NMR spectroscopy. *AAPS Pharmscitech* 3:86–93.
24. Brand RM, Guy RH (1995) Iontophoresis of nicotine in vitro: Pulsatile drug delivery across the skin? *J Control Release* 33:285–292.
25. Wermeling DP, et al. (2008) Microneedles permit transdermal delivery of a skin-impermeant medication to humans. *Proc Natl Acad Sci USA* 105:2058–2063.
26. Valiveti S, et al. (2005) In vivo evaluation of 3-O-alkyl ester transdermal prodrugs of naltrexone in hairless guinea pigs. *J Control Release* 102:509–520.
27. Valiveti S, et al. (2005) In vitro/in vivo correlation of transdermal naltrexone prodrugs in hairless guinea pigs. *Pharm Res* 22:981–989.
28. Ho H, Chien YW (1993) Kinetic evaluation of transdermal nicotine delivery systems. *Drug Dev Ind Pharm* 19:295–313.
29. Tenjarla SN, Allen R, Borazani A (1994) Evaluation of verapamil hydrochloride permeation through human cadaver skin. *Drug Dev Ind Pharm* 20:49–63.
30. D'Amour M, Belanger D (2003) Stability of substituted phenyl groups electrochemically grafted at carbon electrode surface. *J Phys Chem B* 107:4811–4817.